

An Blood Smear Image Based Anemia Recognition System

¹Ching-Lin Wang, ²Meng-Hsiun Tsai, ²Yung-Kuan Chan*, ²Yun-Wei Mao,

²Wei-Chieh Chang, ²Ko-Wei Lin, ³Ching-Hua Chiu

^{1,2}National Chin-Yi University, Taichung, ²National Chung Cheng University, Taichung, Taiwan, R.O.C.

³Department of Bio-Industrial Mechatronics Engineering, National Chung Hsing University, Taichung, Taiwan, R.O.C.

Received 5 Nov 2013; Accepted 23 Dec 2013

Abstract

Anemia diseases have become a worldwide disease. In today's medical technology in diagnose for Red Blood Cells (RBC), medical personnel take the blood sample of patients and through the microscope to observe the blood smear. Blood cell images play an important role in helping diagnosis of the anemia. According to the quantity, size and the contour of the RBC and RBC's disc, the medical can diagnose whether the patient have the symptoms. The Genetic Algorithm Based Parameter Detector (GABPD) helps decide each feature optimal parameter value to recognize the RBC.

The research using different 45 blood smear test images and the total number of the RBC is about 1150. The experimental illustrates the RBC can be correctly segmented by the proposed method and the RBC recognition rate can reach 90%. The conclusion is that the sleep quality of the college students seems poor, and going to PE class turns out to be the main way of doing exercise.

Keywords: RBC, Anemia, Image Segmentation.

Introduction

Anemia diseases have become a worldwide disease. Caused by the body can't produce enough hemoglobin. When the symptom happens, the person will feel weak and exhausted, depressed mood and irritability anxiety. Other symptoms include fatigue, dizziness, syncope, apathy, anxiety. If symptoms are mild, diet therapy can recover, else if symptoms are serious, the need for medical treatment.

For these symptoms, the patient's Red blood cells (RBC) are abnormal and more fragile. In today's medical technology in diagnose for RBC, medical personnel take the blood sample of patients and through the microscope to observe the blood smear. Blood cell images play an important role in helping diagnosis of the anemia. According to the quantity, size and the contour of the RBC and RBC's disc, the professional can diagnose whether the patient have the symptoms. Figure 1 is the blood image including normal and abnormal (Drepanocyte type) cells.

Anemia can separated for many types, such as bad hematopoietic (aplastic anemia, thalassemia), hemolytic

damage (hemolytic anemia) or excessive bleeding (iron deficiency anemia), anemia occur according to different regions and environment, in some Southeast Asian countries, or the Mediterranean countries, the incidence of thalassemia is relatively higher.

Therefore, to develop an automatic computer processing software to process blood smear images can help the professional observe the diseases occur in the parts of body and diagnosis the critical diseases. However, in many blood smear images, red blood cells often overlap and make the recognition difficult. This paper purpose an efficient segmentation method, which combine two methods, erosion and dilation operations method and watershed segmentation. Through the purposed method, we can disconnect the adjacent cells. Then biconcave disk segmentation can achieve from the object histogram equalization and threshold definition. The recognition optimal parameter can obtain through the Genetic algorithm based parameter detector (GABPD). The purposed system can provide the amount of RBC, the biconcave disk area and the RBC type of recognition with useful parameters to help medical do more accurate diagnosis.

*Corresponding author: Yung-Kuan Chan

Tel: 886-4-22857540 ext. 755

Fax: 886-4-22857173

E-mail: mitra.mirsanjari@hotmail.com

Related Work

Image segmentation is one of the most widely studied in image analysis. Many of image segmentation methods have

been proposed such as [1][5]. One of the popular methods for image segmentation is using the statistical model, such as Sector Vector Machines (SVM) or K-means method. But these models have some drawbacks. The performance is not fit in cell segmentation and some models need lots of time training. In the mathematical morphology field, erosion and dilation are one of the classics methods, which used in separate the connectivity of objects in cell images, but the method can't perform well in high overlap ratio cells. Watershed algorithm can perform well on above problems. However, the problem of over-segmentation is usually unavoidable and cells fragment need to be merged. Compare to opening, the execution time cost more.

Based on the above considerations, we present a combining of opening and watershed method for image segmentation in this paper. Only use the watershed algorithm after opening method to minimize the over-segmentation regions and execute time.

Histogram equalization (HE) [6][9] is widely used for the image enhancement. This allows for areas of lower local contrast to gain a higher contrast. However, it tends to change the brightness of an image and cause mean-shift problem. Thus, a considerable amount of research has focused on this subject. In the paper, we use Gamma correction to overcome the drawback of the standard histogram.

Gamma correction

Gamma correction [10][11] is a nonlinear operation used on gray-level images analysis. The gamma correction image be produced through by compute the relation of correspondence between the gray level values and exponent γ . By adjust the exponent γ , when $\gamma > 1$, the brightness regions can be enhanced obviously. On the contrary, the darkness regions be enhanced when $\gamma < 1$. The correspond curve of different γ as in Fig. 1.

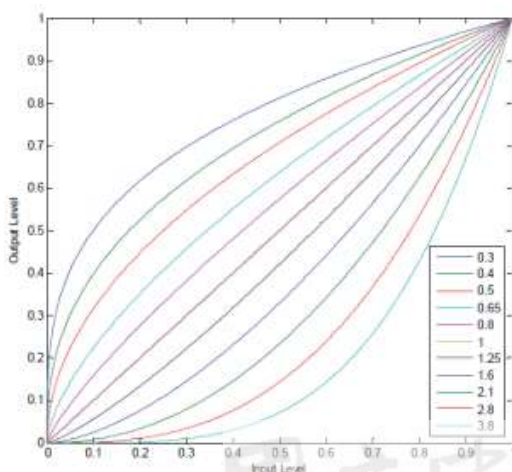


Fig. 1. The correspond curve of different γ

The Gamma correction maps each pixel $I(x,y)$ of the input image into the output $I_g(x,y)$ through a positive exponent γ as:

$$I_g(x,y) = 255 \times \left[\frac{I(x,y) - I_{\min}}{I_{\max} - I_{\min}} \right]^\gamma \tag{1}$$

Where the input image I is assumed to be a gray-level image range from 0 to 255, I_{\max} and I_{\min} stand for the maximum and minimum gray value in I . The difference of γ value is shown in Fig. 2.

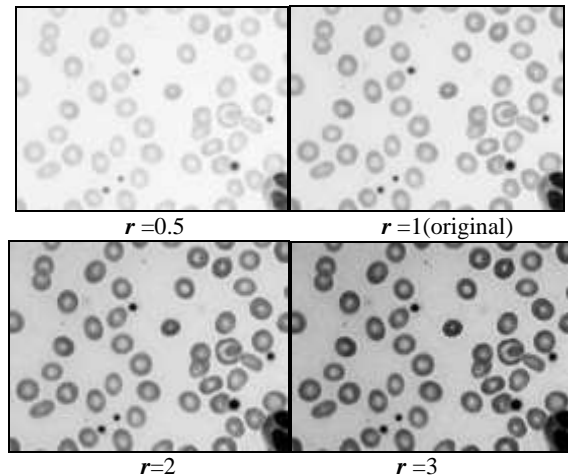


Fig. 2 Gamma correction image with different r

Local Gamma Correction

Uneven illumination always affects image quality seriously in practice. To weaken illumination effect on image quality, we use the Local Gamma Correction method [12]. The image I_g divide into m equal sized blocks $[I_1, I_2, \dots, I_m]$. Then respectively to calculate I_{local} , the function as follows:

$$I_l(x,y) = \begin{cases} \left[\frac{I_g(x,y) - I_{local_{\min}}}{(I_{local_{\max}} - I_{local_{\min}})} \right]^\gamma \times 255 & g(x,y) \in \omega_{q,l} \\ \left[\frac{I(i,j) - I_{local_{\min}}}{(I_{local_{\max}} - I_{local_{\min}})} \right]^{1/\gamma} \times 255 & g(x,y) \in \omega_{q,l} \end{cases} \tag{2}$$

Where I_g is the gamma correction image, I_{local} is the gray level pixel in each blocks correspond $I_g(x,y)$. $I_{local_{\max}}$ and $I_{local_{\min}}$ stand for the maximum and minimum gray value in I_{local} , $I_{local_{mean}}$ stand for the mean value in I_{local} .

Otsu's thresholded method

Otsu's method [13] is used to automatically perform histogram shape-based image threshold, or reduce the gray-level image to a binary image. The procedure is very simple. The algorithm assumes that the image to be thresholded contains two classes of pixels, then decide the optimal threshold to separate two classes by statistical. The Otsu's method is an unsupervised method of automatic threshold selection for different image segmentation. For these reasons, we decided to apply the Otsu's method for image binarization.

The local gamma correction image I_l uses it to specify the threshold T_o . The pixel (i,j) in a binary image $I_{otsu}(i,j)$ is following as:

$$I_{otsu}(i, j) = \begin{cases} 0, & I_l(i, j) \geq T_o \\ 1, & I_l(i, j) < T_o \end{cases} \quad (3)$$

watershed

The watershed algorithm [14][16] is usually implemented by simulating a flooding process. During the processing, the image is taken as a surface of mountainous terrain, and the gray value of each pixel denotes the altitude of that point. In this terrain, there exist deep valleys (minima), high ridges (watershed), and steep or gentle hillsides (catchment basins). Firstly, holes are pierced in each minimum, and then this surface is slowly immersed into a lake. Starting from the minima of lowest altitude, water will progressively fill up the different catchment basins.

Methods of Segmentation

In diagnosis anemia from the blood smear images, some of cells overlap and make the diagnosis difficult. This paper purpose an automatic processing system to help the medical personal which combine two steps, segmentation and recognition. In this chapter we introduce the segmentation part, including RBC segmentation and biconcave disk segmentation.

Then we separate the single cells image and multi-connected cells image from the binary image. In the multi-connected cells, the cells overlapped with others need to be segment. In here, the method of erosion and dilation operations used to disconnect the multi-connected cells. However, if the cells' overlapping region too much, the erosion and dilation operations can't work effectively. Therefore, we use watershed algorithm to solve the above problem. Watershed method can produce good results for separating the high overlapping cells. However, the problem of over-segmentation is usually unavoidable in watershed, so we use the region-merging to combine the fragment regions to meaningful regions after the watershed method.

1. Preprocessing

In the preprocessing step, because a given frequency luminance is more important in distinguishing visual features and grayscale, we convert the original RGB image to grayscale image. Then use gamma correction method and local gamma correction method to improve the contrast of the image. Uneven illumination always affects image quality seriously in practice. If only use the gamma correction on an uneven illumination image, image may have the miscarriage of justice on the binarization step. Local gamma correction image divide into several equal sized blocks. Then respectively use gamma correction method on each region. In this way, the above problem could be solved. To separate the object and background, we use Otsu's method after doing gamma correction and local gamma correction. The Otsu's method is an unsupervised method of automatic threshold selection for image segmentation. After the preprocessing, the original image converts into binary image. Fig. 3 shows the image of the preprocessing steps.

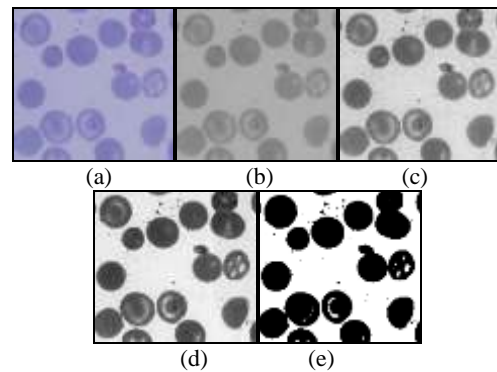


Fig. 3 (a) Original image, (b) Grayscale image, (c) Gamma correction with (b), (d) Local gamma correction with (c), (e) Binary image

2. Cells segmentation

Because of some pictures take from different angles, cells overlap with others, so directly calculate the cells area is inaccurate. Therefore, we separate the single cells image and the multiple-connected cells image and then do the follow-up segmentation methods on the multiple-connected cells image. In order to know each of the single cell area, we filling in the each cell to let the area be stuffed. In this step, we evaluate the single cell area interval from the images. It means when the cells area is located in this interval, we define it single cell. But if the cells area over the interval, we define it multiple-connected cells and need to segment. In here, we sort all of the cells area including single cells and multiple-connected cells. By observation, the value approaching first quartile Q_1 is suitable for single cell area. To consider the different of the blood cell images, we define $Q_1 \pm k \times \sigma$ for the single cell area interval. Where σ stand for the standard deviation of all the cells area in image, k is the constant which optimal value defined by genetic algorithm. The single cells area upper bound T_{SC} and lower bound B_{SC} is defined as:

$$T_{SC} = Q_1 + k \times \sigma \quad (4)$$

$$B_{SC} = Q_1 - k \times \sigma \quad (5)$$

According to the definition of the single cells area, two output images I_{SC} and I_{MC} being generated. That I_{SC} is the image which consists of the single cells area between T_{SC} and B_{SC} . I_{MC} is the image which consists of the cells area over T_{SC} and need segmentation process.

In this section, we use a series of $I_{MC} \ominus b$ and $I_{MC} \oplus b$ operations on the I_{MC} image. Where b stands for the 3×3 structure element of 4-neighbors as 錯誤! 找不到參照來源。 \ominus stand for erosion and \oplus stand for dilation.

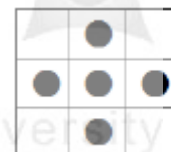


Fig. 4 The 3×3 structure element of 4-neighbors

For I_{MC} , the erosion and dilation operations steps as follows:

Step1: For each overlapping cell do $I_{MC} \ominus b$ iteratively $r/2$ times.

Step2: Then do $I_{MC} \oplus b$ with all the cells. When the disconnect cells intersect with others, retain the intersect regions and avoid connection.

Step3: Repeat step 2 until dilation $r/2$ times.

The number of erosion times is equal to dilation times and it decides based on the single cell radius r . The radius r can be calculated from single cells upper bound area T_{SC} refer as (4). By observation, we define $r/2$ times because of avoiding iteration too many times leading the cells contour deformation.

$$r = \sqrt{T_{SC}/\pi} \quad (6)$$

But not all the multi-connected cells could be separated by the above steps. When the two cells have too much overlapping region, the erosion and dilation operations can't disconnect effectively. Therefore, we use watershed algorithm to solve the above problem.

The watershed algorithm used to **split** the **overlapping object**. Watershed algorithm produces good results for gray level images with different minima and catchment basins. However, the problems of over-segmentation are usually unavoidable, so we use the watershed algorithm on the overlapping cells which can't be separated by erosion and dilation operations. In this way, it can minimize the over-segmentation regions. The I_{MC} image cells can't disconnect by erosion and dilation operations as shown in Fig. 5 (a) and the image after watershed algorithm as shown in Fig. 5 (b).

The watershed algorithm causes the over-segmentation unavoidably. Region-merging can eliminate false boundaries and spurious regions by merging adjacent regions that belong to the same object. Therefore, we merge the over-segmented regions into more meaningful regions. The region-merging steps as follows:

Step1: Calculate each region area from the over-segmentation image.

Step2: Find the min region R_1 in each region.

Step3: Find the minimum region adjacent with R_1 defines to R_2 .

Step4: If $R_1 + R_2 < T_{SC}$, merge the two regions $R_1 | R_2$.

Step5: Repeat step.1~4 until no region can be merged.

The merging image shows in Fig. 5 (c). After the region-merging, the RBC segmentation is finish.

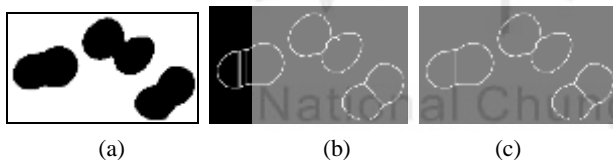


Fig. 5 (a) The image which cells can't be disconnected, (b) The

image of watershed with (a), (c) The image of region-merging with (b)

3. RBC's biconcave disk segmentation

The normal RBC is shaped as biconcave disk, means the disk that is thinner in the center area then on the outside. The professor can diagnose whether the patients' Suffering from anemia diseases by observe the biconcave disk size and the shape of RBC. In this paragraph, we use two steps to extract the disc in the RBC. Because the biconcave disk color is closer to the center area color in grayscale image, some disks may lost by directly using the Otsu's method on the grayscale image. Therefore, we raise the RBC region contrast respectively in order to retain the disc area not lost after binarization.

Object histogram equalization with Otsu

We can get the each RBC location from the chapter 3.1, then respectively to do the function in each RBC region:

$$I'_n(i,j) = 255 \times \frac{I_n(i,j) - I_{min}}{I_{max} - I_{min}} \quad (7)$$

Where I_n is the region n of the RBC with grayscale image, I_{max} and I_{min} stand for the maximum and minimum gray value in I_n . I'_n is the object I_n using histogram equalization.

According the above method, we extract the region inside the RBC. But some of the regions are not the disks instead of the noises. Therefore, according to the difference of gray-level color, we can decide whether the extract regions correspond with the biconcave disk. While the degree of difference is higher than threshold T, we define the region as center area and if lower than T, we define as biconcave disk. The function as follow:

$$T = Mean_{center} - Mean_{disk} + k \times (\sigma_{center} - \sigma_{disk}) \quad (8)$$

Where $Mean_{center}$ and $Mean_{disk}$ is the mean of gray-level pixel in center area and biconcave disk. k stand for the constant and σ_{center} and σ_{disk} stand for the standard deviation of the center area and biconcave disk.

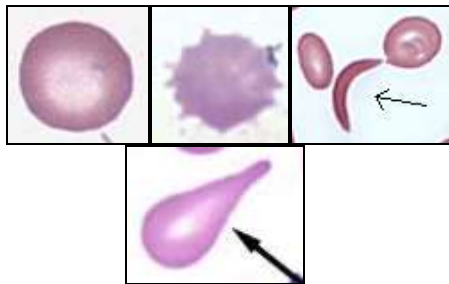
Recognition

In this chapter, we extract the non-overlapping RBC image

I_{SC} and do the shape features recognition.

Fig. is the most common four different types of RBC, normocyte, acanthocyte, drepanocyte and teardrop. If the blood smear images contain the cells except normocyte type, we speculate the patient is likely to infect blood diseases. We define eight features $F_1 \sim F_8$ from each cell and count each RBC types features representative. Then calculate feature distance difference between the identified RBC and each types features

representative. Each feature has its own weight. Through genetic algorithm based parameter detector (GABPD) to decide the optimal weight value for these eight features to help us identify the RBC.



(a) Normocyte (b) Acanthocyte (c) Drepanocyte (d) Teardrop

Fig. 6 The four types of the RBC samples.

The eight features we define as follows:

$$F_1 = A_c / ((\frac{P_c}{2\pi})^2 \times \pi) \tag{9}$$

$$F_2 = A_c / ((\frac{D_c}{2})^2 \times \pi) \tag{10}$$

Where P_c stand for the perimeter and D_c stand for the longest distance of the cell, A_c stand for the cell area. F_1 and F_2 are the area ratio. The value of F_1 and F_2 fall into the range [0,1]. While the value of F_1 or F_2 closer to 1, the cell is closer to roundity. As a rule, the normocyte features F_1 and F_2 values are closer to 1. Compare to normocyte, the acanthocyte feature F_2 and the Drepanocyte feature F_1 usually have lower value.

$$F_3 = L_{q1} / L_s \tag{11}$$

$$F_4 = L_{q3} / L_s \tag{12}$$

We divide the cell of long axis into quartiles, where $q1, q2, q3$ stand for the each point of equal diversion. L_{q1}, L_s, L_{q3} represent the line which perpendicular to the $q1, q2, q3$ and stretch to the edge of the area. L_s is known as short axis. The illustration shows in Fig. 7(a). The difference of F_3 and F_4 can help to separate the teardrop type. As a rule, the teardrop cell difference usually higher and others type difference usually lower.

Feature 5 to 8 is the area out of the cell which through the minimum bounding rectangle to surround the cell. We divide the rectangle to four regions by center of the rectangle stretch the line which perpendicular to the edge. Then count the non-cell pixels from each region and sort these non-cell regions in ascending assigned A_5, A_6, \dots, A_8 . The illustration shows in Fig. (b). The ratio of each regions to the cell area be define as feature F_5, F_6, \dots, F_8 . The purpose of each outside

region divided by the cell area is normalization to [0, 1]. As a rule, the teardrop types and drepanocytes types of features $F_5 \sim F_8$ difference usually higher than normocyte type and acanthocyte type.

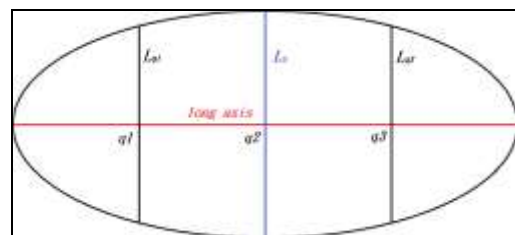
$$F_5 = \frac{A_5}{A_c} \tag{13}$$

$$F_6 = \frac{A_6}{A_c} \tag{14}$$

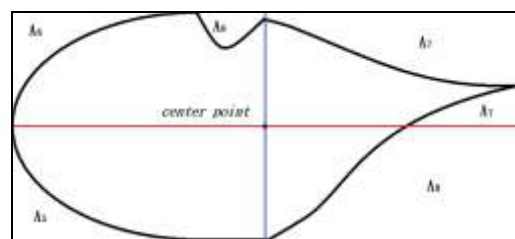
$$F_7 = \frac{A_7}{A_c} \tag{15}$$

$$F_8 = \frac{A_8}{A_c} \tag{16}$$

After computing eight feature values from all the RBC, we take a part of blood cells as the training data. Then, we classify the training data into four types of blood cell. We compute the average value for each feature and each type gain eight average feature values, and then we take these feature values as the type feature. Each feature has different weight, exponential weight and constant weight. By genetic algorithm, we can obtain the best weight of the training data. Then calculate feature distance difference between the RBC and each types features representative from the training data. Then we have four distance difference from the four types of blood. We define the RBC belong minimum distance difference type.



(a)



(b)

Fig. 7 (a) The illustration diagram of the each axis, (b) The illustration diagram of the outside regions

1. Genetic algorithm based parameter detector (GABPD)

In the research, Genetic Algorithm Based Parameter Detector (GABPD) is used to determine the most optimal weights. In this chapter, we define the GABPD and the process of GABPD, including initial, crossover, mutation, selection. The method used on two parts, RBC segmentation and recognition.

In GABPD, an initial population consisting of N chromosomes is specified and then the fitness of each chromosome is calculated for further operation. In order to evolve the optimal solution, the genetic algorithm is used to include repeatedly mutation, crossover and selection operations.

In crossover operation, similarly a random number generator is used to designate N' pairs of chromosomes from the N reserved chromosomes. For each chromosome pair, each bits randomly decide crossover or not.

In mutation operation, for each of the N reserved chromosomes, the GABPD uses a random number generator to specify one bit b for each of s_1, s_2, \dots, s_k . Then, b is replaced by $\neg b$ to generate a new chromosome, where \neg signifies the operator "NOT."

In the selection operation, GABPD select chromosomes as parents from the chromosomes reserved in the previous iteration and the chromosomes are created in the mutation and crossover operations. GABPD iteratively performs these three operations — mutation, crossover, and selection, until one chromosome in the population satisfies the predefined fitness or that the number of iterations is greater than a given number MAX_NO_RUN. Finally, the GABPD extracts the most fitted chromosome and assigns the values decoded from the chromosome to produce the values.

2. RBC segmentation and recognition parameter

In RBC segmentation, the Gamma correction value r_1 , local Gamma correction value r_2 and the single cells area threshold constant k are determined by GABPD. The chromosome is combined with three binary substrings which are $S_{r1}, S_{r2}, S_k, n_{r1}, n_{r2}, n_k$ denote the number of bit of S_{r1}, S_{r2}, S_k and n'_{r1}, n'_{r2}, n'_k are the number that bit value is 1 in the substring. The corresponding relation between each chromosome and parameters r_1, r_2 , and k are defined as follows:

$$\gamma_1 = \frac{n'_{r1}}{n_{r1}} \times 3 \tag{17}$$

$$\gamma_2 = \frac{n'_{r2}}{n_{r2}} \times 3 \tag{18}$$

$$k = \frac{n'_k}{n_k} \times 3 \tag{19}$$

fitness is the Relative Area Error (RAE) [17].

In recognition phase, each feature F_i contains different proportion of weights including constant weight w_i and exponential weight r_i . The chromosome is combined with 16 binary substrings $S_1 \sim S_{16}$, where $S_1 \sim S_8$ stand for the binary string of parameter $r_1 \sim r_8$ and $S_9 \sim S_{16}$ stand for the binary string of parameter $r_9 \sim r_{16}$. Besides, the number of bits of substring are $n_1 \sim n_{16}$, and $n'_1 \sim n'_{16}$ is the number that bit value is 1 in the substring. The corresponding relation between each

chromosome and parameter $w_1 \sim w_8, r_9 \sim r_{16}$ are defined as follows:

$$w_i = \frac{n'_i}{\sum_{i=1}^8 n'_i}, i = 1, 2, \dots, 8 \tag{20}$$

$$r_i = \frac{n'_i}{\sum_{i=9}^{16} n'_i}, i = 9, 10, \dots, 16 \tag{21}$$

The fitness defined as follows:

$$f = \min \{ \sum_{i=1}^8 w_i |F_i - \overline{F_{i,j,k}}|^2 \mid j = 1, \dots, 4, k = 1, 2 \} \tag{22}$$

$F_{i,j,k}$ stands for all the j RBC types, each type divide to k cluster, each cluster has i features. F_i stands for the eight feature in each cells, j stand for the RBC types, total have four types, k stand for each RBC types divide into two cluster.

Experimental Results

We select 45 microscopic images be the test images. For 36 microscopic images are consisted of each 680×512 pixels with 24-bits and else 9 microscopic images consisted of different size pixels with 24-bits and the total number of cells in test images is nearly 1150 cells.

Evaluative criteria

For the RBC segmentation, Misclassification Error (ME) [17], Relative Area Error (RAE) [17], Modified Hausdorff Distance (MHD) [17], and Relative Distance Error (RDE) [18] are often adopted to evaluate the segmentation errors. For the normalization, we not consider the cells which are incomplete or touch to the side.

In the biconcave disk segmentation, there is no other purposed method cab be compared. In here, we use two criteria, Recall and Precision to evaluation our segmentation method, True Positive(TP), False Positive(FP), True Negative(TN), False Negative(FN) define as

TABLE I.

TABLE I. TP, FP, FN, TN DEFINITION

	Ground-truth	
Our method	True	False
True	TP	FP
False	FN	TN

$$\text{Recall} : \frac{TP}{TP + FN} \tag{23}$$

$$\text{Precision} : \frac{TP}{TP + FP} \tag{24}$$

In order to evaluate our proposed methods, the experimental results divide into three parts, RBC segmentation, biconcave disk segmentation and RBC recognition.

RBC segmentation

The test images were used to compute the optimal values of parameters are $r_1=2.7$, $r_2=2.8$, $k=1.6$, Fig. shows five different test images compare to others method (including Level-set [191719, [0] and Fuzzy C-means (FCM) [181]), the figure that contains less number of cells and has the less overlap proportion is shown in Fig. 8 (a), and the performance of level-set and FCM of Fig. 8 (a) are both have ideal performance. In the other hand, the blood cell which has a higher overlap proportion is both hard to use the level-set and FCM to separate the cells and the figure is shown in Fig. 8 (b). However, the method we proposed that can segment well. Compare with other methods, the upper bound of T_{SC} defined in our method will obvious affect the accuracy of segment. If the image that contains more connected RBC or has less cell components, the first quartile Q_1 which the difference of variance will become large, and increase the error amount with T_{SC} and affected the accuracy of segment directly.

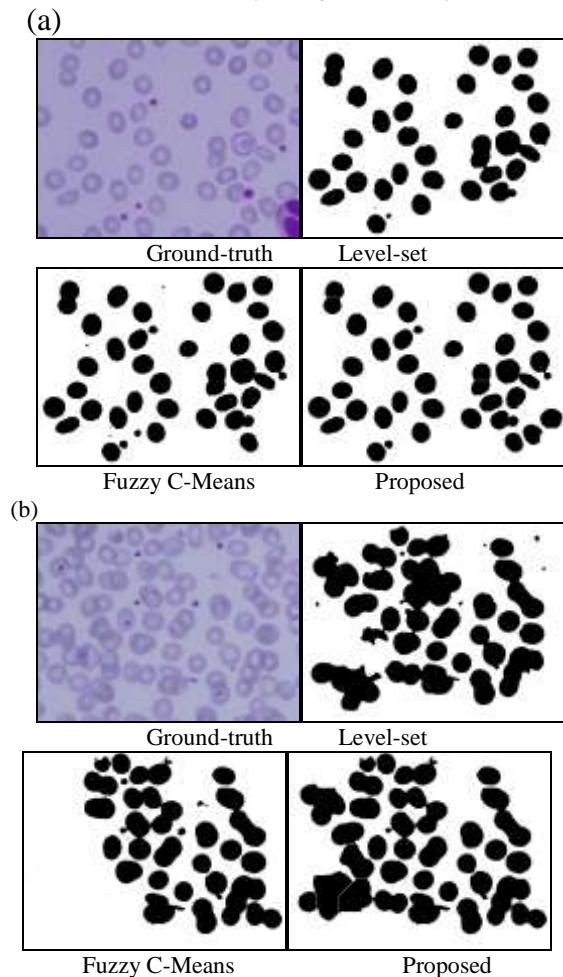


Fig. 8 Different test images segmentation by Level-set, FCM and our proposed method

Fig. 9 demonstrates that the ground-truth image and segmented images by using level-set method, Fuzzy C-means (FCM) method and our proposed RBC segmentation method respectively. In the Fig. 9 (c), level-set method cannot effectively segment the cells and some overlapped cells cannot separate into distinct cells. Although FCM method is more

accurate than level-set method as Fig. 9 (d), it will produce excessive noise. However, our proposed RBC segmentation method as Fig. 9 (e), can more successfully segment the cells than Level-set method and less the noise being generated. T II shows the averages of ME, RAE, MHD and RDE segmenting errors.

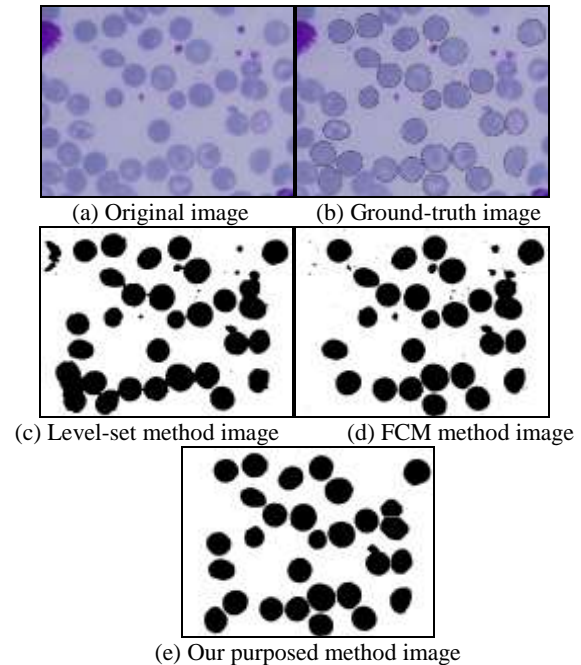


Fig. 9 The ground-truth image and segmented images by using level-set method, FCM method and our proposed method respectively

TABLE II. THE AVERAGE OF ME, RAE, MHD AND

RDE				
	ME	RAE	MHD	RDE
FCM method	0.457	0.298	22.954	21.620
Level-set method	0.451	0.352	20.646	20.680
Our purpose method	0.226	0.107	12.240	14.238

Biconcave disk segmentation

In the biconcave disk segmentation experiment, the system random select 9 images to calculate the sensitivity and accuracy.

Through experiment, the best perform accuracy while $k=1.2$, T III shows different parameter k correspond the average sensitivity and accuracy and

T IV is the parameter $k=1.2$ correspond 9 test images accuracy.

TABLE III. DIFFERENT PARAMETER k CORRESPOND THE ABERAGE ACCURACY

different k	Average recall	Average Precision
$k=1.2$	83.74%	62.20%
$k=1.5$	71.7%	57.26%
$k=2$	57.04%	55.63%
$k=2.5$	36.29%	52.75%

TABLE IV. THE SENSITIVITY AND ACCURACY WITH 9 TEST IMAGES

Test images	Recall(%)	Precision(%)	Test images	Recall(%)	Precision(%)
1	79.72	60.38	6	93.75	68.12
2	90.73	47.06	7	94.61	57.79
3	86.74	50.54	8	50.12	93.13
4	84.02	68.5	9	94.51	48.05
5	79.45	66.29	Avg.	93.92	62.20

RBC recognition

In the recognition experiment, we select total 40 cells for each type of 10 RBC cells to be the training data. Through the GABPD compute the optimal values of $w_1 - w_8$ and $r_1 - r_8$ as T.

TABLE V. THE WEIGHT OF $w_1 - w_8$ AND $r_1 - r_8$

i	w_i	r_i
1	0.1818	0.125
2	0.1591	0.175
3	0.0682	0.2
4	0.1136	0.1
5	0.09	0.15
6	0.1591	0.175
7	0.1136	0.025
8	0.1136	0.05

We get the 16 values w_1-w_8 and r_1-r_8 as identification of parameters. In the experiment, we random select 285 cells to be the test data, the results obtained recognition accuracy up to 90% (256 cells).

Conclusions

For assisting the medical analyzes properties of cells and counts the number of cells, in this paper, an automatic segmentation by erosion and dilation operations and watershed segmentation, and recognition system by using GABPD provide useful data for medical personal do a more accurate determination for the symptom. The experimental results demonstrate that the system can effectively segment cells from an image than other compared methods.

Reference

[1] N. Guo, L. Zeng, Q. Wu, "A method based on multispectral imaging technique for White Blood Cell

segmentation," Computers in Biology and Medicine, Vol. 37, No. 1, pp. 70-76, 2007.

- [2] C. Pan, D. S. Park, S. Yoon, J. C. Yang, "Leukocyte image segmentation using simulated visual attention," Expert Systems with Applications, Vol. 39, No. 8, pp. 7479-7494, 2012.
- [3] Y. K. Chan, P. Y. Pai, C. C. Liu, Y. S. Wang, C.W. Li, L.Y. Wang, "Fluorescence Microscopic Image Cell Segmentation," International Journal of Future Computer and Communication, Vol. 1, No. 1, pp.72-75, 2012.
- [4] A. Genctav, S. Aksoy, S. Onder, "Unsupervised segmentation and classification of cervical cell images," Pattern Recognition, Vol. 45, No. 12, pp. 4151-4168, 2012.
- [5] L. He, Z. Peng, B. Everding, X. Wang, C. Y. Han. K. L. Weiss, W. G. Wee, "A comparative study of deformable contour methods on medical image segmentation," Image and Vision Computing, Vol. 26, No. 2, pp. 141-163, 2008.
- [6] Ming Zeng, Youfu Li, Qinghao Meng, Ting Yang, Jian Liu "Improving histogram-based image contrast enhancement using gray-level information histogram with application to X-ray images," Optik-international Journal for Light and Electron Optics, vol. 123, no. 6, pp. 511-520, 2012.
- [7] K.S. Sim, C.P. Tso, Y.Y. Tan "Recursive sub-image histogram equalization applied to gray scale images," Pattern Recognition Letters, vol.28, no.10, pp.1209-1221, 2007.
- [8] S.D. Chen, A.R. Ramli "Minimum Mean Brightness Error Bi-Histogram Equalization in Contrast Enhancement," IEEE Transactions on Consumer Electronics, vol. 49, no. 4, pp. 1310-1319, 2003.
- [9] H. H. Lin, S. G. Shu, S. W. Kuo, C. H. Wang, Y. P. Chan, S. S. Yu, "Alpha-gamma equalization-enhanced hand radiographic image segmentation scheme," Optical Engineering, pp.107001-1-10.
- [10] D. Zheng, W.J. Park, S.J. Lee, K.A Choi, S.J. Ko, "Histogram partition based gamma correction for image contrast enhancement," IEEE Transactions on Consumer Electronics, pp. 1-4, 2012.
- [11] S.A. A, H. Hassanpour, "A Preprocessing Approach For Image Analysis Using Gamma Correction," International Journal of Computer and Application, vol. 38, no. 12, pp. 38-46, 2012.
- [12] J. Shi, Y.Cai, "A novel image enhancement method using local Gamma correction with three-level thresholding," Information Technology and Artificial Intelligence Conference, vol. 1, pp. 374-378, 2011.
- [13] N. Otsu, "A Threshold selection Method from Gray-Level Histogram," IEEE Transactions on System Man Cybernetics, vol. SMC-9, no. 1, pp.62-66, 1979.
- [14] L. Vincent, P. Soille, "Watersheds in digital spaces: an efficient algorithm based on immersion simulations," IEEE Transaction on Pattern Analysis and machine intelligence, vol. 13, no. 6 pp. 583-598, 1991.

- [15] P. P. Acharjya, D.Ghoshai, "Watershed Segmentation based on Distance Transform and Edge Detection Techniques," International Journal of Computer Applications, vol. 52, no. 13 pp. 583-598, 2012.
- [16] C. L. Orbert, E. W. Bengtsson, and B. G. Nordin, "Watershed Segmentation of Binary Images Using Distance Transformations," The Processing of SPIE — Nonlinear Image Processing IV, Vol. 1902, 1993, pp. 159-170.
- [17] M. Sezgin, and B. Sankur, "Survey over Image Thresholding Techniques and Quantitative Performance Evaluation," Journal of Electronic Imaging, vol. 13, no. 1, pp. 146-165, 2004.
- [18] P. Yan, X. Zhon, M. Shah, and T. C. Wong, "Automatic Segmentation of High-Throughput RNAi Fluorescent Cellular Images," IEEE Transactions on Information Technology in Biomedicine, vol. 12, no. 1, pp. 109-117, 2008.
- [19] Osher, Stanley J.; Fedkiw, Ronald P. (2002). Level Set Methods and Dynamic Implicit Surfaces. Springer-Verlag. ISBN 0-387-95482-1.
- [20] Sethian, James A. (1999). Level Set Methods and Fast Marching Methods: Evolving Interfaces in Computational Geometry, Fluid Mechanics, Computer Vision, and Materials Science. Cambridge University Press. ISBN 0-521-64557-3.
- [181] K. S. Chuang, H. L. Tzeng, S. Chen, J. Wu, T. J. Chen, "Fuzzy c-means clustering with spatial information for image segmentation," Computerized Medical Imaging and Graphics, Vol. 30, No. 1, pp.9-15, 2006.
-



National Chung Hsing University